International Journal of Nanomedicine

Dovepress
open access to scientific and medical research

Open Access Full Text Article

ORIGINAL RESEARCH

Transdermal permeability of triamcinolone acetonide lipid nanoparticles

This article was published in the following Dove Medical Press journal:
International Journal of Nanomedicine

Zhenmiao Qin[1]
Feng Chen[1,2]
Demei Chen[1]
Yong Wang[1,2]
Yinfeng Tan[1,2]
Junfeng Ban[3]

[1]School of Pharmacy, Hainan Medical University, Haikou, People's Republic of China; [2]Hainan Provincial Key Laboratory of R&D of Tropical Herbs, Hainan Medical University, Haikou, People's Republic of China; [3]Guangdong Provincial Key Laboratory of Advanced Drug Delivery Systems, Guangdong Pharmaceutical University, Guangzhou, People's Republic of China

Background: Triamcinolone acetonide (TAA) is an effective and the most commonly used corticosteroid hormone for the treatment of hypertrophic scars (HSs). However, the clinically used dosage has poor tissue permeability and injection safety. By contrast, lipid nanoparticles (LNPs) have the advantage of high affinity for the skin.

Materials and methods: This article describes the preparation of TAA-LNPs using poly(lactic-co-glycolic acid) as a carrier material, which have good biocompatibility and biodegradability. Based on a systematic investigation of its physicochemical properties, a rabbit ear HSs model was established to evaluate the percutaneous permeability of TAA-LNPs in scar tissue in vitro as well as to assess its curative effect and skin irritation.

Results: The results showed that the TAA-LNPs formed uniform and round particles under fluoroscopy and had a complex structure in which a nanoparticle core was surrounded by multiple vesicles. The particles were 232.2±8.2 nm in size, and the complimentary potential was −42.16 mV. The encapsulation efficiency was 85.24%, which is greater than that of other common liposomes and nanoparticles. A test of in vitro scar tissue permeability showed that penetration into scar tissue was twofold and 40-fold higher for TAA-LNPs than for common liposome and commercial suspensions, respectively. The concentration of the absorbed drug effectively inhibited fibroblast proliferation, achieved a therapeutic effect in HSs, and did not stimulate intact or damaged skin.

Conclusion: The preparation of TAA into LNPs for transdermal administration can enhance transdermal permeation performance and the safety of this drug, which is beneficial for the treatment of HSs.

Keywords: lipid nanoparticles, transdermal permeation, triamcinolone acetonide, hypertrophic scars

Introduction

Hypertrophic scars (HSs) are a pathological symptom resulting from excessive deposition of collagen and dermal fibrosis in a local connective tissue after skin dermal injury. They are a common problem in burns, trauma, and postoperative patients which can affect beauty, cause a psychological harm to patients; influence functionality; and cause itching, pain, and other discomfort, preventing patients from living a normal life.[1–4] Triamcinolone acetonide (TAA) is an effective and the most commonly used treatment for HSs.[5] TAA inhibits the proliferation of HSs' fibroblasts and promotes their apoptosis, reducing the degree of dermal fibrosis in the skin to achieve therapeutic effects.[6–8] However, HSs caused by excessive proliferation in the dermis and an increase in the number of fibroblasts led to skin tissue thickening. For this particular skin tissue pathology, drugs that are locally and topically administered do not efficiently penetrate into the depths of the skin through the pathological tissue. This treatment effect is not ideal, and even increasing the amount of drug that is subcutaneously injected or

Correspondence: Yinfeng Tan
Hainan Provincial Key Laboratory of R&D of Tropical Herbs, Hainan Medical University, Haikou 571199, People's Republic of China
Email maksimtan2010@gmail.com

Junfeng Ban
Guangdong Provincial Key Laboratory of Advanced Drug Delivery Systems, Guangdong Pharmaceutical University, Guangzhou 510006, People's Republic of China
Email banjunfeng@163.com

submit your manuscript | www.dovepress.com
Dovepress
http://dx.doi.org/10.2147/IJN.S195769

improving the method of injecting the drug under the scar can produce different degrees of dose-related side effects.[9–12]

Lipid nanoparticles (LNPs) are natural or synthetic lipids that absorb or encapsulate a drug in a lipid nucleus to form a nanodrug delivery system with a particle size of 50–1,000 nm.[13] As novel carriers are used for transdermal administration, LNPs have the following advantages. First, they enhance the stability of the drug. Unlike common liposomes, in LNPs, there is no difference in the drug distribution between the LNPs and the external aqueous phase, which better protects the drug molecules from degradation and significantly improves their stability. Second, LNPs improve the percutaneous penetration of the drug. LNPs have good skin adhesion, easily produce a sealing effect on the skin surface, reduce the loss of water on the skin surface, and promote the transdermal absorption of the drug. Third, LNPs improve skin targeting and reduce adverse reactions.[14–18] Foreign researchers have intensively studied the application of LNPs in transdermal drug delivery systems. Coenzyme Q10, vitamin E, and celecoxib have, for example, been successfully made into topical transdermal formulations.[19–22]

The purpose of this study was to use LNPs as the transdermal drug delivery carrier for TAA to improve its permeability in an HS tissue, to substantially improve the therapeutic effect of the drug on HSs, and to reduce the adverse reactions and side effects caused by an overdose of the clinical medication.

Materials and methods

Materials

Chemicals

TAA was purchased from Tianjin Jinhui Pharmaceutical Co. Ltd. (Tianjin, People's Republic of China) and China National Institute for the Control of Pharmaceutical and Biological Products. Poly(lactic-co-glycolic acid) (PLGA) was purchased from Jinan Daigang Biomaterial Co. Ltd. (Jinan, People's Republic of China). Soy lecithin and egg yolk lecithin were purchased from Advanced Vehicle Technology Pharmaceutical Co. Ltd. (Shanghai, People's Republic of China). Sodium cholate (purity >99%) and urethane were purchased from Guangzhou Weijia Technology Co. Ltd. (Guangzhou, People's Republic of China). Tween-80 was provided by Nanjing Well Pharmaceutical Co. Ltd. (Nanjing, People's Republic of China); α-tocopherol was purchased from Aladdin Reagent Co. (Shanghai, People's Republic of China). Hematoxylin (HE) and alcohol-soluble eosin were supplied by the Department of Pathology and Tissue Science, Guangdong Pharmaceutical University.

The optimal cutting temperature (OCT) frozen slice embedding agent was supplied by the Institute of Vascular Biology, Guangdong Pharmaceutical University. All other chemicals and reagents were commercially available and of reagent grade.

Animals

All animal protocols complied with the Guide for the Care and Use of Laboratory Animals and Institute of Laboratory Animal Resources and were approved by the Institutional Animal Care and Use Committee of Hainan Medical University and Guangdong Pharmaceutical University. Male New Zealand rabbits (2.0–2.5 kg) were purchased from the Laboratory Animal Service Center, Guangzhou University of Chinese Medicine (Guangzhou, People's Republic of China; No SCXK2008-0020). All rabbits had free access to fodder and water.

Preparation of TAA-LNPs

TAA-LNPs were prepared via the film dispersion method. Prescriptions of soybean phospholipids (3.0 g), α-tocopherol (10 mg), sodium cholate, and Tween-80 (1:3, 1.0 g) were placed in a round-bottom flask, adding 10 mL of absolute ethanol to dissolve them. The flasks were connected to a rotary evaporator, and the solvent was evaporated at 40°C, resulting in a yellow and uniform transparent lipid film layer. TAA and PLGA (1:5, 240 mg) were dissolved in acetone–ethanol (8:2, 5 mL)-mixed solvent, quickly injected into a 20-fold 0.5% Tween-80 aqueous solution, and stirred at a room temperature at 600 rpm until the organic solvent volatilized to obtain the TAA nanoparticle suspension. The TAA nanoparticle suspension (the preparation of blank LNPs or common liposomes using distilled water or TAA instead) was placed in a round-bottom flask containing a lipid film layer, and the round-bottom flask was hand-rolled until the dried lipid film on the bottle wall deposited completely. After thorough mixing, it was dispersed using a suitable method (high-speed dispersion and ultrasound or high-pressure homogenization) and passed through a 0.22-μm filter membrane to obtain a TAA-LNPs colloidal solution.

Particle size and ζ-potential analysis

The particle size and ζ-potential of the prepared TAA nanoparticles, common liposomes, and TAA-LNPs were measured directly at 25°C using a DelsaNano™ C particle size and ζ-potential analyzer (Beckman Coulter Inc., Brea, CA, USA). The average particle size, polydispersity index, span, ζ-potential, and electromigration rate were recorded.

Analysis of LNP morphology by transmission electron microscopy (TEM)

The prepared blank LNP colloidal droplets were placed onto the surface of a clean piece of glass that had been sprayed with gold, and the droplet was allowed to dry naturally. The glass was then placed into a low-charge temperature-controlled sample cup, and the temperature was decreased to <10°C. The sample cup was placed in a Phenom G2 Pro benchtop scanning electron microscope (Shanghai, People's Republic of China) to observe the surface morphology at a magnification of 20,500–22,500×.

Analysis of encapsulation efficiency (EE)

The EE of the nanoparticles was determined by reverse dialysis.[23] A 5 mL volume of the prepared TAA-LNP colloidal solution was placed in a 50-mL centrifuge tube and diluted to 20 mL with 0.5% sodium dodecyl sulfate dialysis medium. The two ends of a dialysis bag containing 2 mL of the above dialysis medium were then tied. The mixture was shaken for 10 hours at 100 rpm in a 37°C water bath inside a centrifuge tube. The liquid in the dialysis bag was accurately adjusted by the dialysis medium. The concentration of the free drug was determined by using high-performance liquid chromatography (HPLC; 1260; Agilent Technologies, Santa Clara, CA, USA) using a C_{18} column (5 μm, 250×4.6 mm; Kromasil, Bohus, Sweden) with a mobile phase consisting of a methanol/water mixture (60:40). The flow rate was 1.0 mL/min at 40°C, and the EE was calculated according to the following formula:[24]

$$EE\,(\%) = \frac{1 - W_{free}}{W_{total}} \times 100$$

Preliminary stability

The TAA-LNPs colloidal solution was placed under 60°C and 40°C as high-temperature test conditions, 25°C (room temperature) and 4°C as low-temperature test conditions, and 4,500±500 Lx as light test conditions. The particle size, ζ-potential, and EE of samples were determined on the 5th and 10th to evaluate the preliminary stability of TAA-LNPs (a high-humidity test may not be performed in the liquid state).

In vitro evaluation of transdermal permeation

Four male New Zealand rabbits (Laboratory Animal Service Center, Guangzhou University of Chinese Medicine; SCXK2008-0020) with healthy ears were selected, and their body weight was controlled between 2.0 and 2.5 kg. The HS rabbit ear model was established based on Morris' method.[25–27] The rabbits were anesthetized with 20% urethane 1 g/kg ear vein. Via aseptic operation, a round wound of a diameter of 1 cm was made on the ventral side of the rabbit ear. The wound surface was separated by >1 cm. The whole layer of the skin on the ventral side of the rabbit ear was removed, the perichondrium was completely scraped with a scraping spoon, and the cartilage was retained, with six wounds per ear. The wound was exposed after surgery, and 20 days later, the wound healed and epithelialized to form a scar. Then, the rabbits were sacrificed via the injection of 5 mL of air into the ear margin. Each treated rabbit ear scar sample was fixed in a Franz diffusion cell, and the skin surface was placed such that it faced the supply pool, with the same concentrations of TAA aqueous suspensions, TAA liposomes, and TAA-LNPs. A 20% solution of ethanol in physiological saline was added to the receiving tank, and the water bath was equilibrated to 37°C and set at a fixed speed of 200 rpm. One milliliter of each sample was withdrawn and immediately replaced with an isothermal and equal volume of receiving solution at a specified time, and the sample was then passed through a 0.22-μm filter. The amount of drug in the sample was determined via the HPLC method as described in the "Analysis of encapsulation efficiency" section. The cumulative permeation per area of the scar tissue (Q_n, μg/cm^2) was calculated according to the following formula,[24] with the in vitro transdermal release curve plotted with time (hour) as the abscissa and Q_n (μg/cm^2) as the ordinate:

$$Q_n = \frac{V_n C_n + \sum_{i=1}^{n-1} C_i V_i}{A}$$

where C_n is the drug concentration in the endothelial compartment at different times (mg/mL), C_i is the drug concentration in samples at the final time point (mg/mL), V_n is the volume of the endothelial compartment (18 mL), V_i is the sample volume (1 mL), and A is the effective area of permeation (3.3 cm^2).

Rhodamine B was used as a fluorescent marker to evaluate the depth and strength of the transdermal scar that was penetrated by the LNPs. It was used as a substitute for TAA to prepare rhodamine B-LNPs according to the "Preparation of TAA-LNPs" section so that the mass fraction of rhodamine B in the LNPs was 0.1% (w/w). According to the above transdermal test method, 1 mL of rhodamine

B-LNP suspension was uniformly spread on the rabbit ear surface in the in vivo HS model, and the same concentration of rhodamine B buffer solution (PBS7.0) was used as the control. The skin was removed at 4, 8, and 12 hours, and the preparation solution that had been placed on the scar skin was washed with double-distilled water. The scarred skin tissue was embedded with an OCT embedding agent, and a section with a thickness of 7 μm was cut perpendicular to the scar tissue using a cryostat and then observed under an inverted confocal fluorescence microscope.

Therapeutic study of HSs

The rabbit ear scar model was constructed according to the method in the section "In vitro evaluation of transdermal permeation." After 20 days, a total of 0.5 g of TAA-LNPs was applied to the scar formation of the left ear of the rabbit. In the first group, the treatment was stopped after 10 days of continuous administration; in the second group, the treatment was stopped after 20 days; and in the third group, the treatment was stopped after 30 days. A blank LNP suspension was applied to the scar formation on the right ear of the rabbits, which was used as a negative control.

According to the method described in the section "In vitro evaluation of transdermal permeation," the desired scar tissue was cut out and prepared via dehydration, fixation, and embedding. Tissue sections were then prepared and subjected to staining with HE and Van Gieson's (VG) solution. The distribution of fibroblasts and collagen fibers in the scar tissue was observed in low-power fields using an optical microscope. Ten rectangular fields of view were randomly selected from shallow to deep positions in the tissue, and the densities of the fibroblasts and collagen fibers stained per area of view were analyzed and calculated by using Image-Pro Plus image-processing software (Media Cybernetics, Rockville, MD, USA) and then averaged to obtain the densities of fibroblasts and collagen fibers.

Evaluation of skin irritation

Male New Zealand rabbits with healthy ears were selected, and their body weight was controlled between 2.0 and 2.5 kg. All the rabbits were depilated on both sides of the spine and divided into a single-administered damaged skin group, a single-administered intact skin group, a multiple-administered damaged skin group, a multiple-administered intact skin group, and a saline group to perform single and multiple skin irritation tests.

In the single skin irritation test, 1 g of TAA-LNPs was applied to the left side of each rabbit's back, whereas a solution of blank LNPs was applied to the right side, as a control. The administration site was then covered with a sterile gauze and a nonirritating tape. At 24 hours after administration, residual spread was washed away with warm water, erythema and edema were monitored at the application site for 3 days, and the intensity of the stimulus response was judged according to a scoring and an intensity standard. In the multiple skin irritation test, 1 g of TAA-LNPs was applied to the left side of each rabbit's back once every other day. On the 7th day, a score was determined according to the method used in the single skin irritation test.

Statistical analysis

All results were analyzed and are expressed as the mean ± SD. Differences between groups were assessed via the analysis of variance and the independent samples test using the SPSS software package (SAS Institute, Cary, NC, USA), and $P<0.05$ was considered statistically significant.

Results and discussion

Preparation and characterization of TAA-LNPs

There were some differences among the preparations containing LNPs and common liposomes. Because the LNPs' dispersed phase contains nanoparticles, it is necessary to avoid the destruction of nanoparticles during preparation.[28] In the present study, we investigated the effects of different dispersion processes on particle size distribution and dispersion parameters in LNPs on the basis of an immobilized prescription. The results indicated that different dispersion processes resulted in different dispersion effects on LNPs (Table 1). The high-speed dispersion method had the worst dispersion effect on LNPs, whereas the particle size was not substantially affected even when the speed and time of dispersion were increased. The high-pressure homogenization

Table 1 Results of different dispersion methods and parameters

Dispersion methods	Parameters	Particle size (nm)	PDI	Span
High-speed dispersion	4,000 rpm	509.5±50.1	0.333	3.771
	6,000 rpm	501.7±52.4	0.336	3.586
	8,000 rpm	432.9±28.7	0.361	3.035
Ultrasonic	300 W	377.0±26.4	0.310	3.784
	400 W	350.2±24.2	0.304	3.849
	500 W	321.8±24.4	0.292	3.519
High-pressure homogenization	100 bar	158.2±18.1	0.283	3.547
	200 bar	150.4±19.6	0.260	3.446
	300 bar	141.3±14.7	0.258	3.448

Notes: The high-speed dispersion and ultrasonic breaking times were 5 minutes; the high-pressure homogenization time was 3 minutes. n=3.
Abbreviation: PDI, polydispersity index.

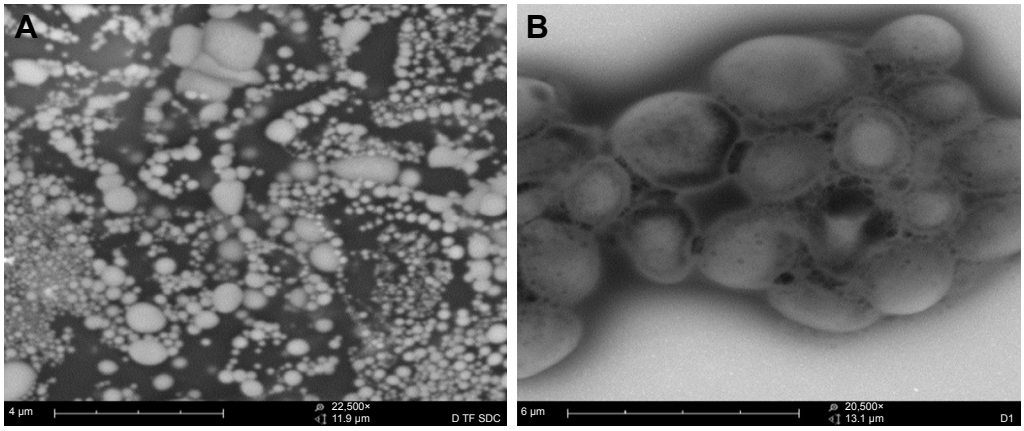

Figure 1 Transmission electron microscopic analysis of the morphology of the LNPs. (**A**) At a magnification of 22,500×; (**B**) at a magnification of 20,500×.
Abbreviation: LNPs, lipid nanoparticles.

method had a better dispersion effect on LNPs, but this method involved dispersion in a high-pressure environment, which may have damaged the structure of LNPs such that the nanoparticles could not form a composite structure with the lipid material. The ultrasonic disruption method achieved better dispersion without destroying the complex structure of LNPs. Therefore, ultrasonic disruption was selected as the dispersion method for the LNPs.

Under TEM, the LNPs had better dispersion properties in the liquid state. The appearance of LNPs was clearly observed (Figure 1A), and the nanoparticles with smaller particle sizes were surrounded by agglomerated lipid membranes, resulting in the formation of a complex structure consisting of a plurality of vesicles with nanoparticles as the core (Figure 1B), confirming the existence of LNPs.

A comparison of LPNs, nanoparticles, and common liposomes revealed that the particle sizes of the LPNs were the largest. Because their structure required a lipid film to encapsulate the nanoparticles, their particle sizes were increased. An analysis of the ζ-potential and electromigration rate made the changes among the three more obvious. The structure of LPNs consisted of a phospholipid membrane containing nanoparticles; therefore, the molecular order of the phospholipid membrane became disordered by the influence of the nanoparticles, and their fluidity was higher than that observed in common liposomes. This indirectly indicated that the deformation of the LPNs depended on the electron migration ability of the ζ-potential layer in the medium, which was impacted by electrophoresis. The EE of LPNs was higher than that of nanoparticles and common liposomes because the lipid material and the nanoparticle solution were incubated at a certain temperature, and the vesicles exhibited a fusion effect after coming into contact with the nanoparticles and recombining into a continuous bilayer around the nanoparticles, thereby increasing the EE of the LPNs (Figure 2; Table 2).[29–31]

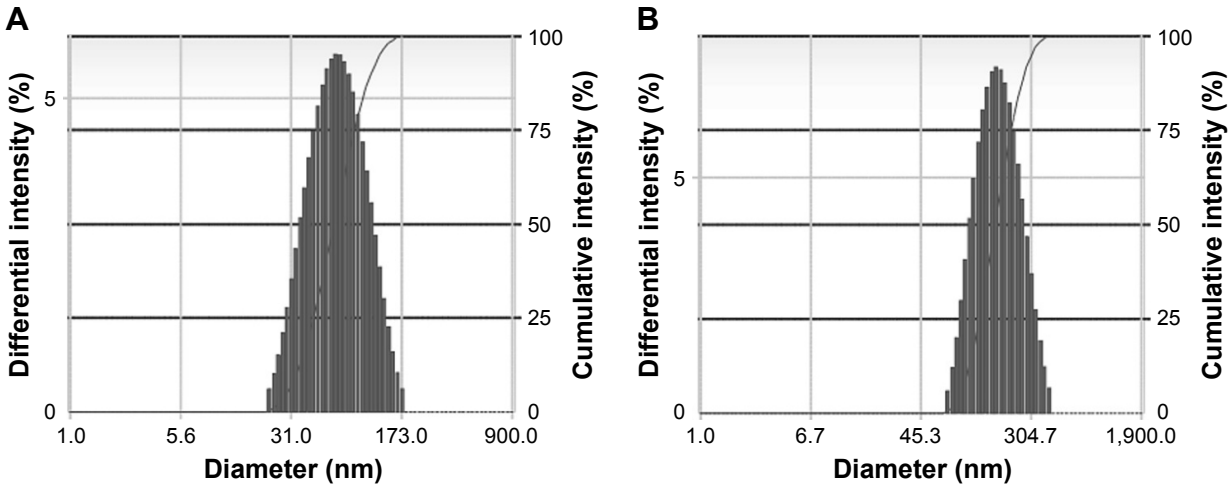

Figure 2 Size distribution of the nanoparticles and LNPs: (**A**) nanoparticles; (**B**) LNPs.
Abbreviation: LNPs, lipid nanoparticles.

Table 2 Characteristics of common liposomes/nanoparticles/LNPs

	Particle size (nm)	ζ-potential (mV)	Electromigration rate ($cm \cdot s^{-1}$)	EE (%)
Common liposomes	183.50±8.82	−33.18	-3.28×10^{-3}	73.10
Nanoparticles	90.97±9.26	6.32	1.79×10^{-5}	59.70
LNPs	232.24±8.24	−42.16	-3.06×10^{-1}	85.24

Abbreviations: LNPs, lipid nanoparticles; EE, encapsulation efficiency.

The preliminary stability evaluation of LNPs was performed by using the influencing factors test according to the guiding principle of the stability test of the preparation, which provided a basis for the subsequent optimization of the preparation process and storage conditions. The results indicated that the LNPs were sensitive to temperature. After 10 days at a room temperature, the particle size and EE changed significantly. When stored at 4°C, the indexes of the LNPs met the requirements. In addition, the effect of light on the LNPs was greater. After 5 days, the properties changed, and the particle size and EE decreased significantly (Table 3). This is because light can accelerate the oxidation of unsaturated fatty acids in phospholipids, converting phospholipids into toxic substances. Therefore, LNPs should be kept in a low-temperature environment (but it is not recommended to freeze them at 0°C) and protected from light to improve their stability.

In vitro evaluation of transdermal permeation

The results of in vitro transdermal permeation of commercially available aqueous suspensions, common liposomes, and TAA-LNPs indicated that the aqueous suspensions barely penetrated into the scar skin within 24 hours and that the amount of permeation was low before 12 hours and began to increase after 12 hours; at 24 hours, the TAA-LNPs penetrated 3.3 times the depth of the common liposomes (Figure 3). These results indicated that the preparations evaluated in this study improved the transdermal permeability of TAA in the scar tissue. This is because the lipid material had a high affinity for the skin, and the nanoparticle-encapsulated drug was less prone to leakage. Once the LNPs had deformed after entering the skin pore, the drug started to be released from the nanoparticle phospholipid membrane, thereby increasing the amount of skin penetration.

Table 3 Preliminary stability of LNPs under different conditions

Conditions	Projects	0th	5th	10th
60°C	Particle size (nm)	142.3	119.4	118.6
	ζ-potential (mV)	−27.21	−21.16	−20.20
	EE (%)	83.94	52.29	37.68
40°C	Particle size (nm)	142.3	133.6	119.1
	ζ-potential (mV)	−35.51	−21.28	−20.60
	EE (%)	83.94	90.54	45.90
25°C	Particle size (nm)	193.0	198.7	196.8
	ζ-potential (mV)	−30.54	−29.57	−27.70
	EE (%)	83.94	76.06	68.99
4°C	Particle size (nm)	116.9	113.0	120.8
	ζ-potential (mV)	−33.83	−35.74	−28.60
	EE (%)	83.94	89.75	88.43
4.500±500 Lx	Particle size (nm)	142.3	123.5	83.3
	ζ-potential (mV)	−27.25	–	–
	EE (%)	83.94	66.45	58.07

Abbreviations: LNPs, lipid nanoparticles; EE, encapsulation efficiency.

An evaluation of fluorescence in sections showed that the amount of rhodamine B in the scar tissue in rabbit ears gradually accumulated over time, and its distribution in the epithelial tissue on the scar surface was clear. Osmotic balance was basically reached after 12 hours (Figures 4 and 5). However, because the scar tissue contains a large number of densely distributed fibroblasts and collagen fibers, the permeability of the scar tissue is lower than that of normal tissue, and the distribution of rhodamine B at the scar was lower than that observed in normal rabbit ears. In contrast, the fluorescence distribution density was higher for the LNPs than for the control group, indicating that the LNPs exhibited

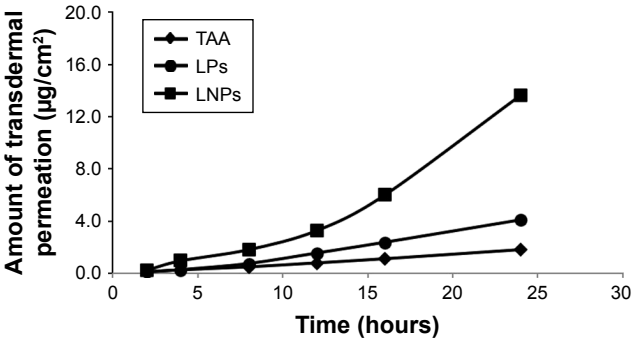

Figure 3 Transdermal permeation curve of aqueous suspensions, common liposomes, and LNPs in vitro.
Abbreviations: TAA, aqueous suspensions; LPs, common liposomes; LNPs, lipid nanoparticles.

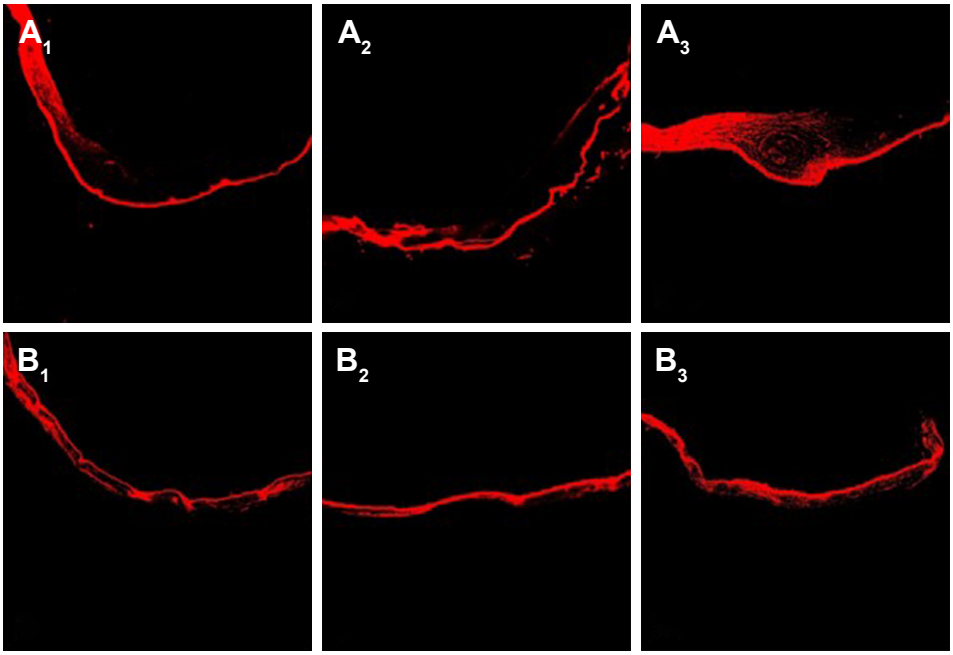

Figure 4 Fluorescence distribution of rhodamine-B in scar tissue in rabbit ears. (**A**$_1$, **A**$_2$, **A**$_3$) LNPs group at 4, 8, and 12 hours, respectively; (**B**$_1$, **B**$_2$, **B**$_3$) the control group at 4, 8, and 12 hours, respectively.
Abbreviation: LNPs, lipid nanoparticles.

an improved ability to penetrate the skin and scar tissue and could, therefore, be used as a transdermal drug carrier for TAA to improve the treatment of HSs.

Therapeutic study of HSs

At 20 days after the operation, the wounds began to exhibit scar hyperplasia. The hyperplasia index of the scar tissue was approximately twofold that of normal rabbit ear skin tissue. At this time, TAA-LNPs began to exert effects. At 10 days after administration, the scar bulge of the wound exhibited no obvious improvement and was red; at 20 days after administration, the color of the scar tissue was lighter, and some of the bulges had begun to become smoother; at 30 days after administration, the color of the scar tissue was similar to that of the surrounding rabbit ear, and the bulges were significantly reduced in height, but redness and swelling were still observed in the center of the scar. In the negative control group treated with the blank matrix, the thickness of the scar was significantly higher than that observed in the intervention group. Although the scar area was not enlarged, the swelling of the scar tissue block was more severe, and clear granuloma could be observed by the naked eye (Figure 6).

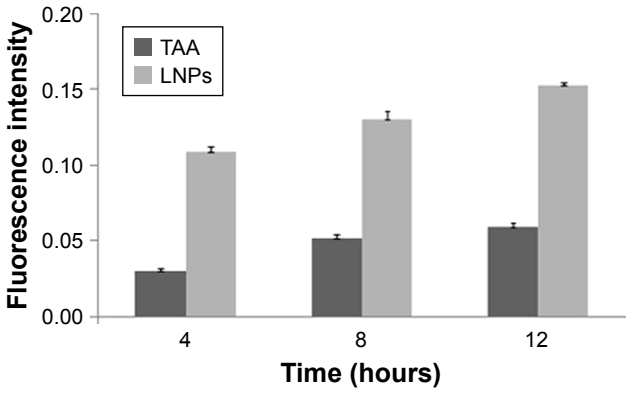

Figure 5 Fluorescence density of rhodamine-B in scar tissue in rabbit ears after 4–12 hours.
Abbreviations: TAA, aqueous suspensions; LNPs, lipid nanoparticles.

The distribution of fibroblasts and collagen fibers observed in HE- and VG-stained sections showed that there were large numbers of dense and irregularly arranged fibroblasts and collagen fibers in the scar tissue in the model group. At 20 days after intervention, the scar tissue thickness was lower in the drug-administered group than in the model group, and the arrangements of fibroblasts and collagen fibers were relatively neat and loose (Figures 7 and 8). The densities of fibroblasts and collagen fibers were also lower (Figure 9). Our overall observations of this phenomenon and the results of calculations confirmed that the TAA-LNPs prepared in this study achieved therapeutic effects by inhibiting the proliferation of HS fibroblasts and promoting their apoptosis and by reducing the degree of dermal fibrosis in the skin.

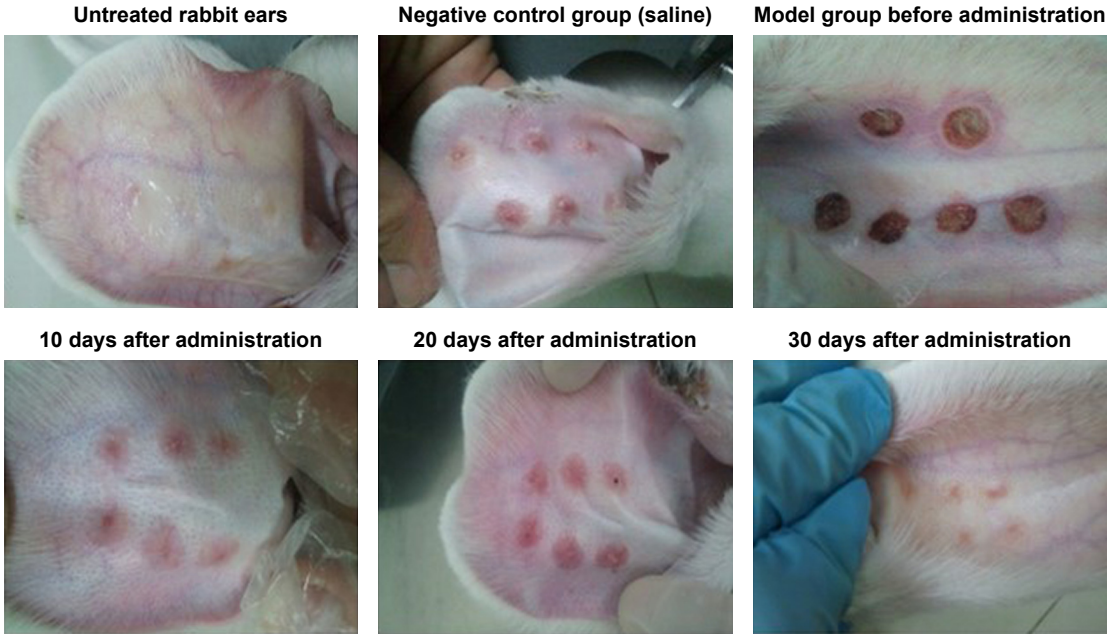

Figure 6 Overall observation of scarring after surgery.

Evaluation of skin irritation

The results of the single skin irritation test showed that, in normal rabbit skin, the irritation response of TAA-LNPs was zero and that TAA-LNPs were less irritating to intact skin after 24 hours (Table 4). This result indicated that a single administration of TAA-LNPs produced little irritation in the skin. The results of a multiple skin irritation test indicated that TAA-LNPs and blank matrix produced less irritation in intact skin, with the response scores on the first day 0.17 and 0, respectively (neither was statistically significant). The damaged skin presented mild irritation on the first and third days, and this reaction disappeared on the fifth day.

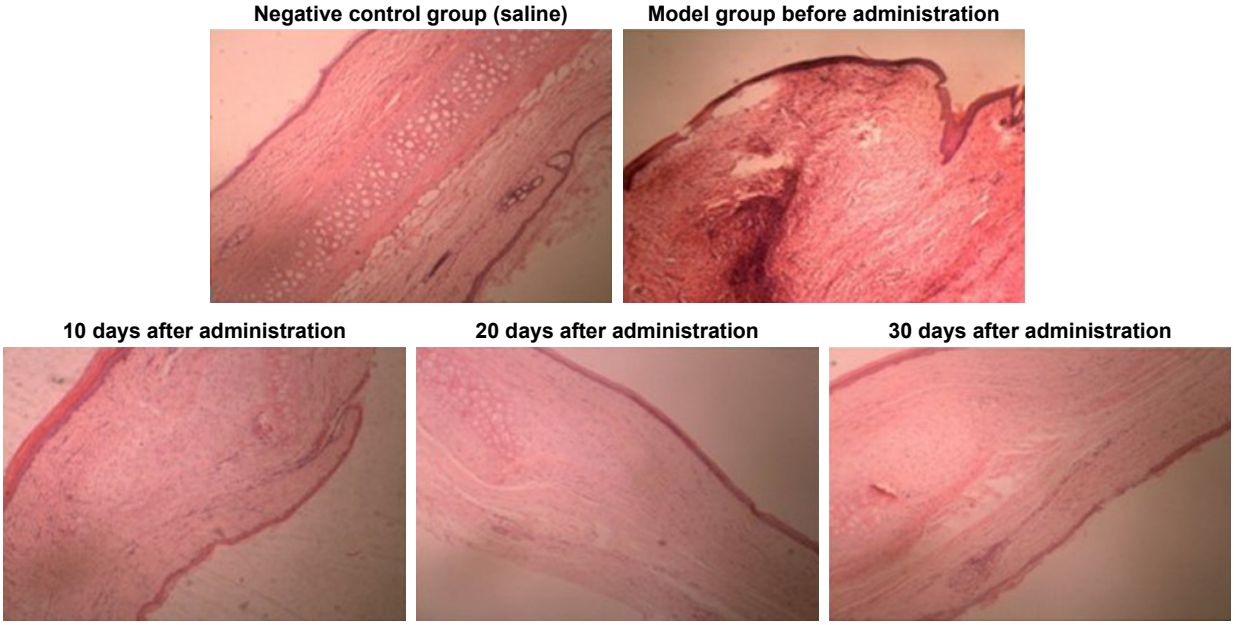

Figure 7 HE-stained slices of rabbit ears obtained from different groups treated with HSs (4×10).
Abbreviations: HE, hematoxylin; HSs, hypertrophic scars.

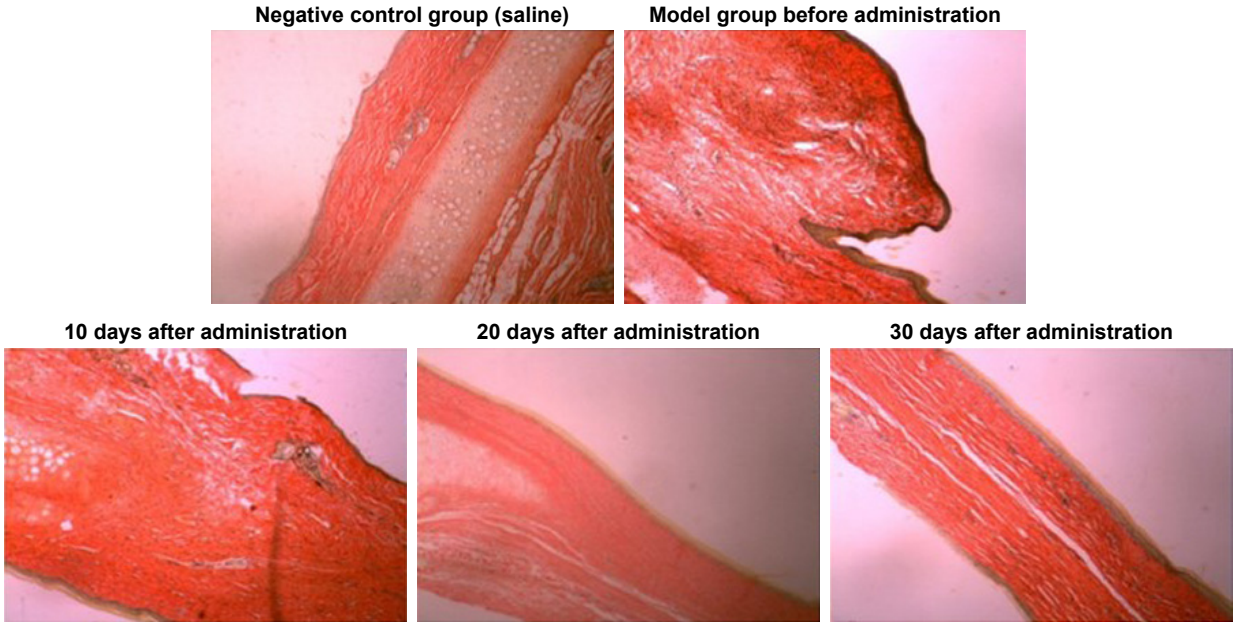

Figure 8 The VG-stained slices of rabbit ears obtained from different groups treated with HSs (4×10).
Abbreviations: VG, Van Gieson's solution; HSs, hypertrophic scars.

The control skin exhibited mild irritation only on the first day (Table 5). Therefore, the response scores of the two were not significantly different. In summary, the TAA-LNPs may mildly irritate damaged skin after multiple administrations, and the residual solution left after a previous application should, therefore, be removed when multiple administrations are required to reduce this effect. In the HS tissue with unfinished epithelialization, it is important to pay attention to whether a treatment will stimulate the scar tissue when applied in multiple administrations.

Conclusion

As a novel transdermal drug carrier, LNPs have high affinity for skin and produced no irritation. Furthermore, they easily

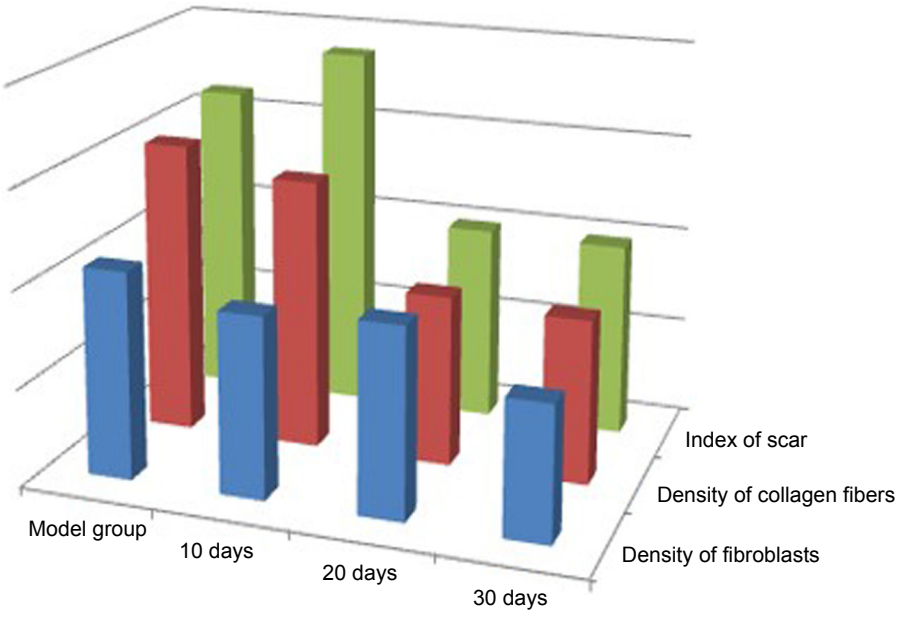

Figure 9 Various index values of scar tissue observed after administration.

Table 4 Scores of single skin irritation tests performed using TAA-LNPs

Conditions	Time (hours)	Average score	Significant difference	
			Differences within the groups	Differences between groups
Intact skin				
Test skin	24	0.00	$P>0.05$	$P>0.05$
	48	0.00		
	72	0.00		
Control skin	24	0.00		
	48	0.00		
	72	0.00		
Damaged skin				
Test skin	24	0.67	$P>0.05$	$P>0.05$
	48	0.17		
	72	0.00		
Control skin	24	0.00		
	48	0.00		
	72	0.00		

Abbreviations: TAA, triamcinolone acetonide; LNPs, lipid nanoparticles.

produced a sealing effect on the skin surface, prevented water dispersion, and improved the rate of penetration rate of the drug into the skin. In this study, LNPs were used as transdermal delivery carriers for TAA. In the in vitro scar permeability test, the percutaneous penetration ability was higher for TAA-LNPs than for common liposomes and commercial suspensions tested under the same conditions. The drug mainly concentrated on the surface layer of the skin and in the shallow layer of the dermis, which can prevent excessive drug from entering the blood circulation, where it could cause adverse reactions, while exerting local curative effects. The preliminary results of pharmacodynamic experiments showed that the absorption of TAA-LNPs into the scar tissue achieved an effective inhibitory concentration and an inhibited fibroblast proliferation in vitro. The results indicated that the TAA-LNPs prepared by the treatment evaluated here effectively prevented excessive scar hyperplasia, and it is, therefore, expected that this approach will be developed into a novel topical preparation for treating HSs.

Table 5 Scores of multiple skin irritation tests performed with TAA-LNPs

Condition	Time (days)	Average score	Significant difference	
			Differences within the groups	Differences between groups
Intact skin				
Test skin	1	0.17	$P>0.05$	$P>0.05$
	3	0.00		
	5	0.00		
	7	0.00		
Control skin	1	0.00		
	3	0.00		
	5	0.00		
	7	0.00		
Damaged skin				
Test skin	1	0.67	$P>0.05$	$P>0.05$
	3	0.50		
	5	0.00		
	7	0.00		
Control skin	1	0.50		
	3	0.00		
	5	0.00		
	7	0.00		

Abbreviations: TAA, triamcinolone acetonide; LNPs, lipid nanoparticles.

Acknowledgment

This work was supported by the R&D Team for Formulation Innovation (Grant Number: 2015CXQX150), the Innovation and Strong School Project of Guangdong Pharmaceutical University (Grant Number: 2015KQNCX077), and the Guangdong "Climbing" Program for Undergraduates (Grant Numbers: PDJH2O17B0266, pdjh2018b0263, and pdjh2018b0265).

Disclosure

The authors report no conflicts of interest in this work.

References

1. Sandy SU, Kenneth AA, Jeffrey SD. Keloids and hypertrophic scars: review and treatment strategies. *Semin Cutan Med Surg*. 1992;18(2):159–171.
2. Rabello FB, Souza CD, Farina Júnior JA. Update on hypertrophic scar treatment. *Clinics (Sao Paulo)*. 2014;69(8):565–573.
3. Ledon JA, Savas J, Franca K, Chacon A, Nouri K. Intralesional treatment for keloids and hypertrophic scars: a review. *Dermatol Surg*. 2013;39(12):1745–1757. doi:10.1111/dsu.12346
4. Brissett AE, Sherris DA. Scar contractures, hypertrophic scars, and keloids. *Facial Plast Surg*. 2001;17(4):263–272. doi:10.1055/s-2001-18827
5. Sadeghinia A, Sadeghinia S. Comparison of the efficacy of intralesional triamcinolone acetonide and 5-fluorouracil tattooing for the treatment of keloids. *Dermatol Surg*. 2012;38(1):104–109. doi:10.1111/j.1524-4725.2011.02137.x
6. Morgan SM, Sherry SC. Combination treatment of CO_2 fractional laser, pulsed dye laser, and triamcinolone acetonide injection for refractory keloid scars on the upper back. *J Cosmet Laser Ther*. 2013;15(3):166–170. doi:10.3109/14764172.2013.780448
7. Gerd GG, Hans CK, Tatiana P, et al. Hypertrophic scarring and keloids: pathomechanisms and current and emerging treatment strategies. *Mol Med*. 2011;17(1–2):113–125. doi:10.2119/molmed.2009.00153
8. Finken MJJ, Mul D. Cushing's syndrome and adrenal insufficiency after intradermal triamcinolone acetonide for keloid scars. *Eur J Pediatr*. 2010;169(9):1147–1149. doi:10.1007/s00431-010-1185-8
9. Sandy SU, Arndt KA, Dover JS. Keloids and hypertrophic scars: review and treatment strategies. *Semin Cutan Med Surg*. 1999;2(18):159–171.

10. Xi C, Lihua P, Jianqing G. Novel topical drug delivery systems and their potential use in scars treatment. *Asian J Pharm Sci*. 2012;7(3):155–167.
11. Mofikoya BO, Adeyemo WL, Abdus-salam AA. Keloid and hypertrophic scars: a review of recent developments in pathogenesis and management. *Nig Q J Hosp Med*. 2007;17(4):134–139.
12. Meseci E, Kayatas S, Api M, Boza A, Cikman MS. Comparison of the effectiveness of topical silicone gel and corticosteroid cream on the pfannenstiel scar prevention – a randomized controlled trial. *Ginekol Pol*. 2017;88(11):591–598. doi:10.5603/GP.a2017.0107
13. Tapeinos C, Battaglini M, Ciofani G. Advances in the design of solid lipid nanoparticles and nanostructured lipid carriers for targeting brain diseases. *J Control Release*. 2017;264:306–332. doi:10.1016/j.jconrel.2017.08.033
14. Zhang YT, Han MQ, Shen LN, Zhao JH, Feng NP. Solid lipid nanoparticles formulated for transdermal aconitine administration and evaluated in vitro and in vivo. *J Biomed Nanotechnol*. 2015;11(2):351–361.
15. Charoenputtakhun P, Opanasopit P, Rojanarata T, Ngawhirunpat T. All-trans retinoic acid-loaded lipid nanoparticles as a transdermal drug delivery carrier. *Pharm Dev Technol*. 2014;19(2):164–172. doi:10.3109/10837450.2013.763261
16. Singla SK, Sachdeva V. Current and emerging lipid-based systems for transdermal drug delivery. *Ther Deliv*. 2015;6(9):1063–1070. doi:10.4155/tde.15.66
17. Gaur PK, Mishra S, Purohit S. Solid lipid nanoparticles of guggul lipid as drug carrier for transdermal drug delivery. *Biomed Res Int*. 2013;2013:750690.
18. Pardeike J, Hommoss A, Müller RH. Lipid nanoparticles (SLN, NLC) in cosmetic and pharmaceutical dermal products. *Int J Pharm*. 2009;366(1–2):170–184. doi:10.1016/j.ijpharm.2008.10.003
19. Al-Rasheed NM, Al-Rasheed NM, Abdel Baky NA, et al. Prophylactic role of α-lipoic acid and vitamin E against zinc oxide nanoparticles induced metabolic and immune disorders in rat's liver. *Eur Rev Med Pharmacol Sci*. 2014;18(12):1813–1828.
20. Papp K, Menter MA, Raman M, et al. A randomized phase 2b trial of baricitinib an oral JAKl/JAK2 inhibitor, in patients with moderate-to-severe psoriasis. *Br J Dermatol*. 2016;174(6):1266–1276. doi:10.1111/bjd.14403
21. Punwani N, Burn T, Scherle P, et al. Downmodulation of key inflammatory cell markers with a topical Janus kinase 1/2 inhibitor. *Br J Dermatol*. 2015;173(4):989–997. doi:10.1111/bjd.13994
22. Chen J, Wei N, Lopez-Garcia M, et al. Development and evaluation of resveratrol, Vitamin E, and epigallocatechin gallate loaded lipid nanoparticles for skin care applications. *Eur J Pharm Biopharm*. 2017;117:286–291. doi:10.1016/j.ejpb.2017.04.008
23. Morales JO, Valdés K, Morales J, Oyarzun-Ampuero F. Lipid nanoparticles for the topical delivery of retinoids and derivatives. *Nanomedicine (Lond)*. 2015;10(2):253–269. doi:10.2217/nnm.14.159
24. Ban J, Zhang Y, Huang X, et al. Corneal permeation properties of a charged lipid nanoparticle carrier containing dexamethasone. *Int J Nanomedicine*. 2017;12:1329–1339. doi:10.2147/IJN.S126199
25. Morris DE, Wu L, Zhao LL, et al. Acute and Chronic animal models for excessive dermal scarring: quantitative study. *Plast Reconstr Surg*. 1996;100(3):674–682.
26. Gong YF, Zhang XM, Yu J, et al. Effect of recombinant human endostatin on hypertrophic scar fibroblast apoptosis in a rabbit ear model. *Biomed Pharmacother*. 2017;91:680–686. doi:10.1016/j.biopha.2017.04.116
27. Wang Q, Dong Y, Geng S, Su H, Ge W, Zhen C. Photodynamic therapy inhibits the formation of hypertrophic scars in rabbit ears by regulating metalloproteinases and tissue inhibitor of metalloproteinase-1. *Clin Exp Dermatol*. 2014;39(2):196–201. doi:10.1111/ced.12265
28. Parhi R, Suresh P. Preparation and characterization of solid lipid nanoparticles-a review. *Curr Drug Discov Technol*. 2012;9(1):2–16.
29. Kathe N, Henriksen B, Chauhan H. Physicochemical characterization techniques for solid lipid nanoparticles: principles and limitations. *Drug Dev Ind Pharm*. 2014;40(12):1565–1575. doi:10.3109/03639045.2014.909840
30. Nandini PT, Doijad RC, Shivakumar HN, Dandagi PM. Formulation and evaluation of gemcitabine-loaded solid lipid nanoparticles. *Drug Deliv*. 2015;22(5):647–651. doi:10.3109/10717544.2013.860502
31. Lütfi G, Müzeyyen D. Preparation and characterization of polymeric and lipid nanoparticles of pilocarpine HCl for ocular application. *Pharm Dev Technol*. 2013;18(3):701–709. doi:10.3109/10837450.2012.705298